Journal of the Chinese Society of Mechanical Engineers, Vol.47, No.5, pp 445~457 (2026)

Jarring Force Analysis and Dynamic Characteristics Study of Hydraulic Drilling Jar

Jialin Tian*, Long Ran**, Jianbo Yang*, Junyang Song** and Chunjian Huang**

Keywords: Jar, Hydraulic cylinder, Jarring force, Dynamics, Drilling tools.

Abstract

With the more complex downhole conditions, stuck drilling often occurs in downhole drilling system. In order to quickly deal with the stuck drilling accident and resume drilling operation, this study proposes an up-and-down integrated hydraulic jar while drilling. Theoretical analysis is conducted on the collision force based on its working characteristics, and motion simulation analysis of the jar couple is carried out. The dynamic characteristics of the drill string system are determined by establishing multi-degree-of-freedom model for downhole axial vibrations, and subsequently analyzing the resulting drill string vibration loads and related parameters. Analysis results demonstrate that in order to obtain a better effect of unlocking, the hydraulic drilling jar should be installed as close as possible to the stuck point, and the force acting on hydraulic drilling jar should be increased. Finally, the experimental verification is conducted to complete the tensile and compression experiments of both upstroke and downstroke generated by the drilling jar. The maximum relative error of the upper impact collision force was 6.9616%, and the average relative error was 5.6185%; while the maximum relative error between theoretical calculation results and experimental values of lower impact collision force was 6.7199%, and the average relative error was 6.85%. All relative errors are within the reasonable range. The reliability of the theoretical calculations is confirmed through a comparison between the experimental and theoretical results.

Introduction

Oil and gas will remain the main source of primary energy in the world for a long time (Jin et al., 2024). In the development of oil and gas resources, due to the improper design of borehole trajectory, the wrong operation of downhole operations and the complex geological structure (Tian et al., 2023), drilling tools are often stuck (Kelly, 2022; Mao et al., 2015). At this point, it needs to be unstuck by field personnel to resume drilling operations (Li, 2019). A jar can be used to release the stuck drill when conventional methods are not effective. The jar is a kind of downhole tool which can make a strong impact on the stuck drill by the elastic deformation of the drill string and relieve the stuck drill accident very effectively (Yin et al., 2014). While drilling, the jar is a tool that can be used to release stuck along with the drilling string. When the stuck occurs in the well, the jar can be started immediately to produce a violent release force to the stuck point to achieve the purpose of releasing stuck (Mcgill et al., 1968). With the increase of complex well conditions such as deep well, ultra-deep well and horizontal well, the application of jar while drilling is becoming more and more extensive (Li, 2014).

The size of the jar force is directly related to the performance of the jar. In the beginning, people basically used the method of combining elastic wave theory and dynamics to study the jarring force. Skeem et al. (1979) regard the drill string as an elastic rod, and based on the one-dimensional elastic wave theory, establish a jar release model. In this model, the jar serves as a release-and-catch mechanism allowing energy to be transferred to the upper collars after the jar triggers or releases and to the lower collars and stuck point after impact. Based on the model established by Skeem, Kalsi et al. (1987) added factors such as friction, nonlinearity and damping into consideration, and obtained the laws of vibration displacement, velocity, acceleration and magnitude of vibration force at each axis position of drill string under the action of jolt release force. Based on the Skeem theory, Zhang et al. (1998) also calculated the impulse, stuck point displacement and jarring force generated in the process of jarring release in detail, providing a basis for adjusting the overpull of the jar according to the actual situation during the jarring

Paper Received April, 2025. Revised May, 2025. Accepted July, 2025. Author for Correspondence: Long Ran.

* *Professor, Department of Mechanical Engineering, Southwest Petroleum University, Chengdu, Sichuan 610500.*

** *Graduate Student, Department of Mechanical Engineering, Southwest Petroleum University, Chengdu, Sichuan 610500.*

operation. Aarrestad et al. (1994) analyzed the distribution of vibration load on the drill string during jar release, and pointed out that the traditional calculation method of friction in extended reach Wells and horizontal Wells would lead to large errors in the calculation results, and further studied the law of the influence of heavy drill pipe on the jar release force. Liu et al. (2008; 2008) used the Rayleigh method in the process of shock and vibration, combined with the propagation theory of elastic waves, to establish the dynamic model of jar release, and completed the dynamic discussion of the bench test of the hydraulic hammer.

With the development of finite element software and computer technology, finite element method has also been applied to the calculation of jolt force (Deng et al., 2008). Askew (1986) used the finite element method to numerically simulate the jolting operation under different drill assemblies and different well depths to solve the variation laws of displacement, velocity and released force. Newman et al. (2009) considered a single drill pipe as a rod element with multiple degrees of freedom, established a finite element mechanical model according to actual drilling conditions, and simulated and solved the dynamic response of various locations. Li (2019) used ANSYS to simulate various responses of the bottom drill pipe under longitudinal impact, and compared it with the theoretical analytical solution to verify the reliability of the analytical solution.

At the same time, Han et al. (2015) developed a double-acting mechanical hydraulic jar while drilling. The mechanical locking of the tool can avoid false vibration operation, and the hydraulic delay mechanism of up and down stroke enhances the effect of jar and unstuck. Guo et al. (2009) designed a fully mechanical air drilling jar suitable for underbalanced air drilling. Aiming at the service life of the jar while drilling. Hu et al. (2016) developed a hydraulic continuous jar, which is used in high-temperature and high-pressure working environments. Feng et al. (2024) proposed a bidirectional hydraulic jar, which successfully solved the problem of stuck drill during oilfield operations and verified the feasibility of removing stuck mechanical shock absorbers. Pan et al. (2010) specifically solved the bending strength ratio between the upper joint and the converter joint, found the cause of the fracture of the jar joint, and reduced the zero point of the axial stress of the drill string to the drill collar by optimizing the drill assembly. Fan et al. (2013) optimized the design of the hydraulic damping mechanism, the core component of the hydraulic jar, improved the material of the damping part and improved the surface treatment of the damping part.

In this paper, hydraulic drilling jar with reasonable structure and superior performance is designed. The working mechanism and characteristics are analyzed through theory, simulation and experiment. At the same time, the hydraulic drilling jar solves the problem of unchangeable vibration force after the conventional jar is inserted into the well, realizes the drilling continuity and operation convenience, greatly reduces the processing time of stuck drill accident, and reduces the drilling production cost.

Working mechanism

The hydraulic drilling jar is mainly composed of four parts: drive assembly, upper strike assembly, lower strike assembly and balance assembly. The structure diagram of hydraulic drilling jar is shown in Figure 1.

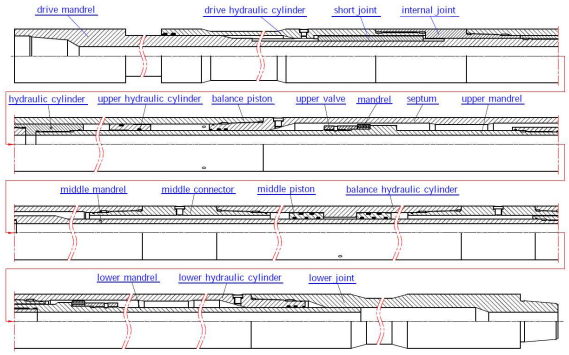

Fig. 1. The structure diagram of the hydraulic drilling jar

The hydraulic drilling jar has an upper and lower hydraulic cylinder, and following is an explanation of how it works with up-jar impact motion.

Hydraulic drilling jars are generally in a fully open state into the well, so before its upstroke operation, it is necessary to reduce the hook or top drive load, and lower the drill string to make the hydraulic jar in a retracted state. When the drilling process is stuck and needs an upward impact, the drill string should be lifted up. When the upper edge of the valve is moved to the pressurized zone, mandrel system drives the valve to move slowly upward. The elastic potential energy of the upper drill string and the mandrel system keeps increasing.

After lifting the suspension weight to the set parameters, stop the hook or top drive. Under the action of elastic deformation force drive up, the upper valve to continue to go up. Until the lower edge of the upper valve leaves the pressurized zone, a large amount of elastic potential energy stored is released instantaneously.

The upper drill string and mandrel system elastic contraction, and the upper valve accelerated upward motion, until the internal joint collides violently with the short joint, a strong upward impact force is generated on the short joint, which is transmitted through the cylinder system, the lower joint to the lower drill string assembly, and then to the stuck point.

The down-jar impact is similar to the up-jar impact. After the down-jar impact motion is completed,

try to lift the drill string up. If the drill string up still cannot lift successfully, it is necessary to gradually increase the release force of the down-jar impact and knock it down several times.

During normal drilling, hydraulic drilling jar is located in the drill string system and acts similarly to drill pipe. However, due to the position of the tool in drill string system, the state of hydraulic drilling jar is different, so the tool can be stressed differently. Figure 2 and Figure 3 show the axial force and torque transfer of the jar while drilling when it is located above the neutral point (the position in the drill string system that is neither strained nor compressed).

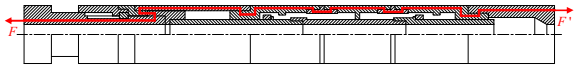

Fig. 2. Tensile axial force transfer diagram of hydraulic drilling jar during normal drilling

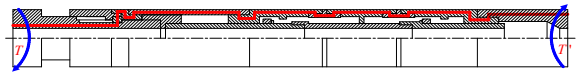

Fig. 3. Tensile torque transfer diagram of hydraulic drilling jar during normal drilling

When the hydraulic jar is located below the neutral point, the axial force and torque transfer are shown in Figure 4 and Figure 5.

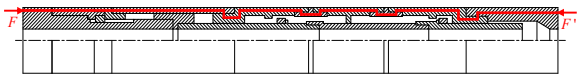

Fig. 4. Axial pressure transfer diagram of hydraulic drilling jar during normal drilling

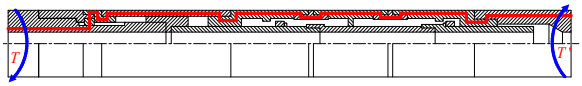

Fig. 5. Torque transfer under pressure diagram of hydraulic drilling jar during normal drilling

Comparing Fig. 2 and Fig. 4, it can be found that the transmission of axial force will be different due to the different states of hydraulic drilling jar. When hydraulic drilling jar is in tension, the axial force is transmitted from the up-jar couple. When hydraulic drilling jar is under compression, the axial force is transmitted by the down-jar couple. However, by comparing Fig. 3 and Fig. 5, it can be found that the torque transmission is not changed, although the state of tool is different. The torque is transmitted to the cylinder system by the mandrel and cylinder of the drive assembly. For most cases, the hydraulic drilling jar is above the neutral point and in tension in the drill string system.

Jarring force of hydraulic drilling jar

Theoretical model

In order to better solve the regular of tension and pressure which hydraulic drilling jar is subjected to, the following assumptions are proposed for the calculation model (Sun et al., 1997):

(1) Both the mandrel and hydraulic cylinder system are regarded as elastomers with continuous and uniform mass.

(2) In the collision process, the conversion of kinetic energy and elastic potential energy is considered, and the loss of other energy is ignored.

(3) Shock couple collision is completely inelastic, there is no elastic rebound after collision.

The axial force transmission of hydraulic drilling jar in tension is shown in Figure 6, where the dark blue part is the pressure holding area. The axial force is transmitted to the upper mandrel through the driving mandrel, and then to the upper cylinder through the valve body pressure on the upper mandrel, and then to the lower drill string.

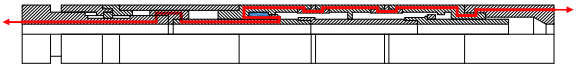

Fig. 6. Diagram of up-jar impact process

At the moment of the up-jar impact, the collision between the internal joint and the short joint is equivalent to the collision of two elastic rigid bodies. At this time, the upper impact collision force F_{sj} obtained by mandrel system is:

$$F_{sj} = K_2\delta_3 = \sqrt{2K_2U_{yg}} = \sqrt{K_2m_2}\cdot\frac{m_1}{m_1+m_2}F_s\left(\frac{v_1}{A_3E_1}+\frac{L_{sj}}{m_1v_1}\right) \quad (1)$$

where K_2 is the axial stiffness coefficient of the cylinder system, δ_3 is the deformation of cylinder system under up impact force, U_{yg} is the elastic potential energy of the cylinder system, m_1 is the quality of mandrel system, m_2 is the quality of the cylinder system, F_s is the upstroke release force, v_1 is the longitudinal propagation velocity of elastic wave in mandrel system, A_3 is the equivalent cross-sectional area of the mandrel system, E_1 is the elastic modulus of mandrel system material and L_{sj} is the upstroke.

According to the assumption, the shock is a completely inelastic collision. The law of conservation of momentum:

The axial force transmission of hydraulic drilling jar under pressure is shown in Figure 7, where the dark blue part is the pressure holding area.

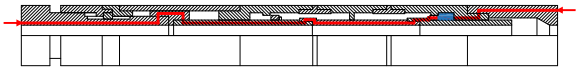

Fig. 7. Diagram of down-jar impact process

Similarly, the lower impact collision force F_{xj} can be obtained as:

$$F_{xj} = \sqrt{K_2m_2}\cdot\frac{m_1}{m_1+m_2}F_x\left(\frac{v_1}{A_3E_1}+\frac{L_{xj}}{m_1v_1}\right) \quad (2)$$

where L_{xj} is the downstroke.

For this multi-rigid body collision model of

hydraulic drilling jar, the Cartesian 3D coordinates of colliding rigid body mass block i and the Eulerian angle reflecting orientation of rigid body mass block are used as the generalized coordinates:

$$\begin{aligned} q_i &= \left[x, y, z, \psi, \theta, \varphi\right]_i^T \\ q &= \left[q_1^T, \cdots, q_n^T\right]^T \end{aligned} \tag{3}$$

The kinetic simulation software uses the Lagrange multiplier method to establish the equations of motion for the multi-rigid body system:

$$\frac{d}{dt}\left(\frac{\partial T}{\partial \dot{q}}\right)^T - \left(\frac{\partial T}{\partial q}\right)^T + g_{\dot{q}}^T \mu + f_q^T \rho = Q \tag{4}$$

where T is the kinetic energy of the collision system, Q is the generalized force matrix of the system, μ is the incomplete constrained matrix, ρ is the complete constrained matrix and $\dot{q}$ is the generalized velocity matrix of the system.

For systems that are not fully constrained: $g(q,\dot{q},t)=0$. For systems that are fully constrained: $f(q,t)=0$.

For hydraulic drilling jar collision in this study, the compensation method and impact function method are used to define collision. Generally, the impact function method is used to calculate the collision force, which includes the elastic force generated by mutual ingestion between the two collision bodies, and the damping force generated by the relative velocity.

The expression of the impact function method is:

$$F_{impact} = \begin{cases} k\left(q_0 - q\right)^e \\ -c_{\max} \cdot \left(dq/dt\right) \cdot step\left(q, q_0 - h, 1, q_0, 0\right) & q \le q_0 \\ 0 & q > q_0 \end{cases} \tag{5}$$

Avoid the discontinuity of the damping force during the collision, where the step function is

$$step = \begin{cases} h_0 & x \le x_0 \\ h_0 + \left(h_1 - h_0\right)\left(\dfrac{x - x_0}{x_1 - x_0}\right)^2 \left(3 - \dfrac{2\left(x - x_0\right)}{x_1 - x_0}\right) & x_0 < x < x_1 \\ h_1 & x \ge x_1 \end{cases} \tag{6}$$

where k is the shock couple stiffness coefficient, q_0 is the initial distance, q is the distance of collision body, e is the collision index of collision mass, $c_{\max}$ is the maximum damping coefficient, dq/dt is the change rate of the distance with time and h is the depth of ingestion between two colliders.

Jarring force results analysis

According to the structural design parameters and working mode of hydraulic drilling jar, the gravity coefficient is set to 9.8, and material properties of each component are edited. The constraints and motion pairs are established, and finally the load and power drive are added to kinematic pairs.

For the impact surface of the shock couple, the elastic index is set to 1.5, and the maximum damping coefficient is 0.1%~1% of impact stiffness coefficient. When the sticking accident occurs, the hydraulic cylinder system of hydraulic drilling jar is equivalent to being fixed to the earth. In the simulation software, the lower end face of lower joint is fixed to the earth. The mandrel system is set as a sliding pair for the earth. The driving mandrel, upper mandrel, middle mandrel and lower mandrel are simplified into a whole that is fixed to each other. Similarly, the driving cylinder, hydraulic cylinder, upper hydraulic cylinder, balance hydraulic cylinder, lower hydraulic cylinder and the lower joint are simplified into a whole that is fixed to each other. Tension is added to the end face of the driving mandrel. Finally, the simulation analysis and calculation are carried out on the sliding pair.

According to the design parameters of Φ168 hydraulic drilling jar in this study, combined with the relevant arithmetic parameters, as shown in Table 1.

Table 1. Relevant arithmetic parameters

Parameters	Unit	Value
Elastic modulus of mandrel	Pa	2.1×10^{11}
Poisson ratio of mandrel material	\	0.26
Mandrel material density	kg/m^3	7850
Kinematic viscosity of oil	mm^2/s	14.396
Density oil of hydraulic oil	g/mm^3	8.7×10^{-10}
Maximum OD of upper mandrel core	mm	4.44
Maximum OD of lower mandrel core	mm	4.42
Total length of mandrel system	m	8.612
Mass of mandrel system	kg	344.432
Upper cylinder holding pressure length	m	0.150
Upper impact stroke	m	0.135
Lower cylinder holding pressure length	m	0.135
Lower impact stroke	m	0.125
Mass of cylinder system	m	569.917
Total length of cylinder system	kg	6.07
Elastic modulus of the cylinder	Pa	2.1×10^{11}

The collision force is calculated by substituting the relevant parameters and structure parameters of hydraulic drilling jar into the calculation model. Solve the upper impact collision force by taking the tension force on the mandrel in the range of 300kN~800kN, and solve the lower impact collision force by taking the pressure on the mandrel in the range of 100kN~350kN. So, the collision force corresponding

to the force on mandrel of hydraulic drilling jar are calculated. The results of the theoretical calculation and simulation comparison are shown in Figure 8 and Figure 9.

Analysis of the theoretical calculation results and simulation values in Fig. 8 and Fig. 9 shows that the collision force generated by the hydraulic drilling jar is positively correlated with the force acting on mandrel. As the force acting on mandrel increases, the collision force generated by it also increases. Since there is no influence of the drilling tool combination, the length of the mandrel is limited and elastic deformation produced is small. The collision force generated by the hydraulic drilling jar is not much different from the force acting on its mandrel, so the force acting on the hydraulic drilling jar is one of the key factors to generate the collision shock force.

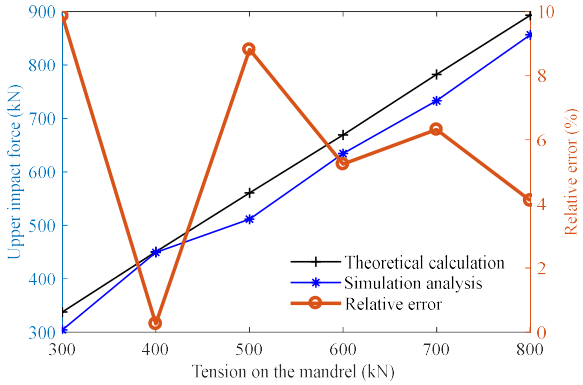

Fig. 8. Relationship between tensile force on the mandrel and upper impact force

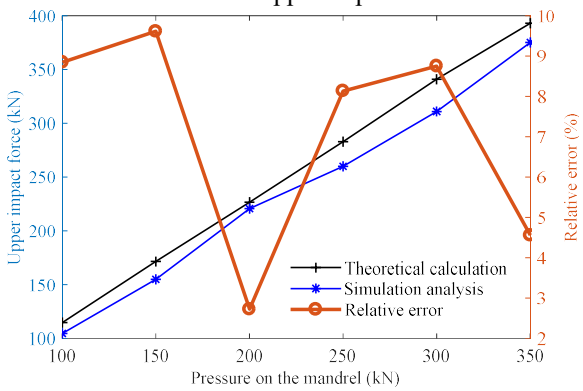

Fig. 9. Relationship between pressure on the mandrel and lower impact force

According to Fig. 8 and Fig. 9, comparing the theoretical calculation results with simulation solution values, the overall simulation value of collision impact force is smaller than the theoretical calculation results. The reason is that, in the theoretical calculation, only the conversion of kinetic and elastic potential energy during the process; the theoretical calculation value ignores the deformation generated by collision; ignores the damping and conversion loss of internal energy. However, the maximum relative error between theoretical calculation and simulated value of the upper impact collision force is 9.8621%, and the average relative error is 5.7665%; the maximum relative error between theoretical calculation and experimental value of lower impact collision force is 9.6123%, and the average relative error is 7.1042%; all are within the reasonable range of relative error, which confirms the reliability of the theoretical calculation and the simulated value.

Axial dynamics analysis

When the drill is stuck, the jar while drilling is started to unlock the stuck operation. Combined with the actual drilling conditions, the actual movement of the drill string system under the combined action of its own properties, external forces and various boundary conditions is quite complicated, which is not easy to be expressed by reasonable mathematical expression. Therefore, according to the existing research results on axial vibration of drill string, the main influencing factors were analyzed and the secondary influencing factors were ignored to simplify the model (Zhao et al., 2007; Tian et al., 2019; Li et al., 2004). Therefore, the following hypotheses were proposed:

(1) Both the drill string system and the hydraulic drilling jar are elastic deformable and have approximately the same material properties.

(2) The drilling string system is located in a vertical well with an inclination of 0° and the borehole axis of the drilling string system is coaxial.

(3) Ignoring the transverse and torsional vibration of the drill string system in the well, only the axial vibration is considered.

(4) Both the drill string system and the borehole boundary surface are rigid surfaces and are in uniform contact.

(5) The effects of buoyancy and temperature change of drilling fluid are ignored, and the effects of torsion on axial length change of drilling string are ignored.

(6) The drill string system is long enough that the simplification of the upper boundary conditions does not affect the propagation of the drill string vibration waves.

(7) The kelly, drill pipe, drill collar and drill bit of the drill string system are regarded as the equivalent mass lumps respectively, and the mass blocks of the drill collar contain both the weight drill pipe and the centralizer.

(8) When the hook load indicator reading reaches the design value of the jolt release force, it remains fixed, assuming no displacement.

Dynamical model

Based on the simplified assumptions of above model and combined with the actual drilling conditions, the equivalent dynamic vibration model of is established for kelly bar, drill pipe, drill collar, hydraulic drilling jar, integrated drill collar and drill bit contained in the drill string system.

The multi-degree-of-freedom drill string dynamics model established in Figure 10. In the figure, m_1, m_2, $m_2 \cdots m_n$, m_d, m_j, m_{ds}, m_b and y_k, y_1, $y_2 \cdots y_n$, y_d, y_j, y_{ds}, y_b represent the equivalent mass and axial displacement of kelly bar, drill pipe 1, drill pipe $2 \cdots$ drill pipe n, drill collar, tool, integrated drill collar and drill bit. k_1, $k_2 \cdots k_n$, k_d, k_j, k_{ds}, k_b and c_1, $c_2 \cdots c_n$, c_d, c_j, c_{ds}, c_b represent the axial stiffness and damping between equivalent mass blocks. F_h is the force of hook acting on the kelly bar. F_j is the axial shock force output by hydraulic drilling jar. F_f is the viscous resistance caused by sticking.

Newton 's second motion law is applied to the discrete equivalent mass block m_i of drill string.

For kelly bar, drill bit, hydraulic drilling jar and integrated drill collar are separately:

$$\begin{cases} i=k, F_k = m_k g - F_h \\ i=b, F_b = m_b g \\ i=j, F_j = m_j g - F_j(t) \\ i=ds, F_{ds} = m_{ds} g + F_f \end{cases} \tag{8}$$

The differential formula of motion is derived:

$$\begin{cases} m_k \ddot{y}_k - c_1(\dot{y}_1 - \dot{y}_k) - k_1(y_1 - y_k) = m_k g - F_h \\ m_b \ddot{y}_b + c_b(\dot{y}_b - \dot{y}_{ds}) + k_b(y_b - y_{ds}) = m_b g \\ m_j \ddot{y}_j - c_{ds}(\dot{y}_{ds} - \dot{y}_j) + c_j(\dot{y}_j - \dot{y}_d) \\ -k_{ds}(y_{ds} - y_j) + k_j(y_j - y_d) = m_j g - F_j(t) \\ m_{ds} \ddot{y}_{ds} - c_b(\dot{y}_b - \dot{y}_{ds}) + c_{ds}(\dot{y}_{ds} - \dot{y}_j) \\ -k_b(y_b - y_{ds}) + k_{ds}(y_{ds} - y_j) = m_{ds} g + F_f \end{cases} \tag{9}$$

By sorting out the above equation, the axial dynamic model of each equivalent mass point of drill string system can be obtained as follows:

$$\begin{cases} m_t \ddot{y}_k - c_1(\dot{y}_1 - \dot{y}_k) - k_1(y_1 - y_k) = m_k g - F_h \\ m_1 \ddot{y}_1 - c_2(\dot{y}_2 - \dot{y}_1) + c_1(\dot{y}_1 - \dot{y}_k) - k_2(y_2 - y_1) \\ + k_1(y_1 - y_k) = m_1 g \\ m_2 \ddot{y}_2 - c_3(\dot{y}_3 - \dot{y}_2) + c_2(\dot{y}_2 - \dot{y}_1) - k_3(y_3 - y_2) \\ + k_2(y_2 - y_1) = m_2 g \\ \vdots \\ m_n \ddot{y}_n - c_d(\dot{y}_d - \dot{y}_n) + c_n(\dot{y}_n - \dot{y}_{n-1}) - k_d(y_d - y_n) \\ + k_n(y_n - y_{n-1}) = m_n g \\ m_d \ddot{y}_d - c_j(\dot{y}_j - \dot{y}_d) + c_d(\dot{y}_d - \dot{y}_n) - k_j(y_j - y_d) \\ + k_d(y_d - y_n) = m_d g \\ m_j \ddot{y}_j - c_{ds}(\dot{y}_{ds} - \dot{y}_j) + c_j(\dot{y}_j - \dot{y}_d) - k_{ds}(y_{ds} - y_j) \\ + k_j(y_j - y_d) = m_j g - F_j(t) \\ m_{ds} \ddot{y}_{ds} - c_b(\dot{y}_b - \dot{y}_{ds}) + c_{ds}(\dot{y}_{ds} - \dot{y}_j) - k_b(y_b - y_{ds}) \\ + k_{ds}(y_{ds} - y_j) = m_{ds} g + F_f \\ m_b \ddot{y}_b + c_b(\dot{y}_b - \dot{y}_{ds}) + k_b(y_b - y_{ds}) = m_b g \end{cases} \tag{10}$$

Suppose that the initial boundary conditions are:

$$\begin{cases} y_i(t=0) = 0 \\ \dot{y}_i(t=0) = 0 \end{cases} \tag{11}$$

where i is the node unit of each equivalent mass block from kelly bar to drill bit of drill string system.

The axial drill string state vector $\mathbf{z}$ is:

$$\begin{aligned} \mathbf{z} &= (y_k, \dot{y}_k, y_1, \dot{y}_1, \cdots, y_n, \dot{y}_n, y_d, \dot{y}_d, y_j, \\ &\dot{y}_j, y_{ds}, \dot{y}_{ds}, y_b, \dot{y}_b)^T \\ &= (z_1, z_2, z_3, z_4, \cdots, z_{m-7}, z_{m-6}, z_{m-5}, \\ &z_{m-4}, z_{m-3}, z_{m-2}, z_{m-1}, z_m)^T \end{aligned} \tag{12}$$

where $m = 2n + 8$ is the order-number of the system state variables.

By dividing the left and right sides of Equation (10) by the equivalent mass m_i at the same time, the Equation (12) can be written in the form of a first-order differential equation group:

$$\begin{cases} \dot{z}_1 = z_2 \\ \dot{z}_2 = g - \dfrac{c_1}{m_k}(z_2 - z_4) - \dfrac{k_1}{m_k}(z_1 - z_3) - \dfrac{F_h}{m_k} \\ \dot{z}_3 = z_4 \\ \dot{z}_4 = g + \dfrac{c_1}{m_1}(z_2 - z_4) + \dfrac{k_1}{m_1}(z_1 - z_3) \\ -\dfrac{c_2}{m_1}(z_4 - z_6) - \dfrac{k_2}{m_1}(z_3 - z_5) \\ \vdots \\ \dot{z}_{m-6} = g + \dfrac{c_d}{m_d}(z_{m-8} - z_{m-6}) + \dfrac{k_d}{m_d}(z_{m-9} - z_{m-7}) \\ -\dfrac{c_j}{m_d}(z_{m-6} - z_{m-4}) - \dfrac{k_j}{m_d}(z_{m-7} - z_{m-5}) \\ \dot{z}_{m-5} = z_{m-4} \\ \dot{z}_{m-4} = g + \dfrac{c_j}{m_j}(z_{m-6} - z_{m-4}) + \dfrac{k_j}{m_j}(z_{m-7} - z_{m-5}) \\ -\dfrac{c_{ds}}{m_j}(z_{m-4} - z_{m-2}) - \dfrac{k_{ds}}{m_j}(z_{m-5} - z_{m-3}) - \dfrac{F_j(t)}{m_j} \\ \dot{z}_{m-3} = z_{m-2} \\ \dot{z}_{m-2} = g + \dfrac{c_{ds}}{m_{ds}}(z_{m-4} - z_{m-2}) + \dfrac{k_{ds}}{m_{ds}}(z_{m-5} - z_{m-3}) \\ -\dfrac{c_b}{m_{ds}}(z_{m-2} - z_m) - \dfrac{k_b}{m_{ds}}(z_{m-3} - z_{m-1}) + \dfrac{F_f}{m_{ds}} \\ \dot{z}_{m-1} = z_m \\ \dot{z}_m = g + \dfrac{c_b}{m_b}(z_{m-2} - z_m) + \dfrac{k_b}{m_b}(z_{m-3} - z_{m-1}) \end{cases} \tag{13}$$

The axial stiffness k_i between each two equivalent mass blocks is:

$$k_i = \frac{\pi E_i (D_i^2 - d_i^2)}{4 l_i} \tag{14}$$

where i is the equivalent node of drill string, E_i is the elastic modulus of drill string material, D_i is the outer diameter of equivalent node of drill string, d_i is the inner diameter of equivalent node of drill string and l_i is the length of equivalent node of drill string.

Along the axial direction of drill string, the damping of material structure is usually small, and the viscous damping of drilling fluid is large. Therefore, in order to accurately analyze the axial vibration characteristics of downhole tool, it is necessary to consider the influence of viscous damping. For the convenience of calculation, Rayleigh damping is used in this paper. The damping matrix of equivalent mass block of drill string system can be expressed by mass matrix and stiffness matrix. The damping matrix is:

$$\mathbf{C} = \alpha\mathbf{M} + \beta\mathbf{K} \tag{15}$$

where α and β are two proportional constant coefficients, which are valued by the relevant results of reference in this paper.

The mass m_i of the drill string equivalent node block in the drill string system is:

$$m_i = \frac{\pi}{4}\rho_i l_i (D_i^2 - d_i^2) \tag{16}$$

where ρ_i is the material density at equivalent node of drill string.

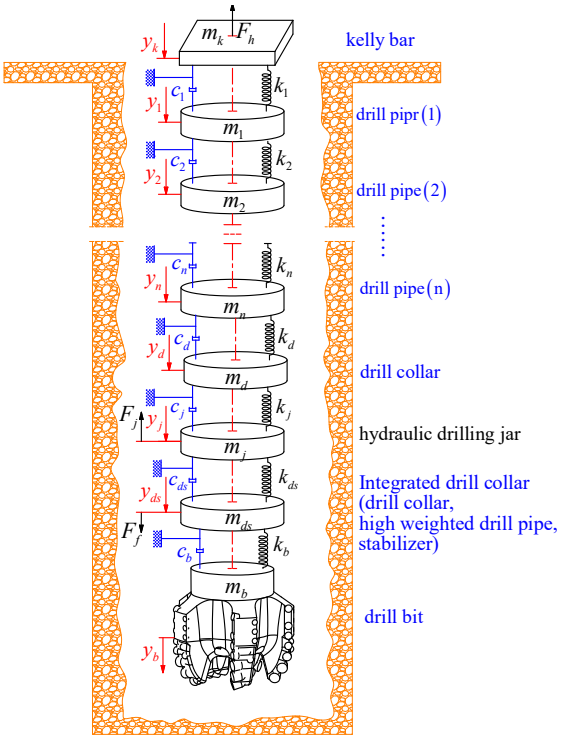

Fig. 10. Diagram of down-jar impact process

Case study

The established multi-degree-of-freedom drill string dynamics model is numerically analyzed, and the critical calculation parameters are shown in Table 2.

Table 2. Axial vibration related parameters

Parameters	Unit	Value
Mass of drill collar	kg	1.2×10^4
Mass of hydraulic drilling jar	kg	915
Mass of integrated drill collar	kg	3×10^4
Mass of drill bit	kg	85
Outer diameter of high weight drill pipe	m	0.127
Inner diameter of high weight drill pipe	m	0.0762
Outer diameter of drill collar	m	0.1588
Inner diameter of drill collar	m	0.714
Coefficient α	\	0.1
Coefficient β	\	0.001
Length of drill string joint	m	9.5
Stuck resistance	kN	600

It is assumed that stuck point is located at the depth of 4500 m, and hydraulic drilling jar is installed 100 m away from the stuck point. In the axial direction of the whole drill string system dynamics model, the upper joint of the kelly bar belongs to the upper boundary condition. When the hook load reaches the design value of specified jarring release force, keep fixed, that is, there is no displacement change on the upper boundary. The jarring load generated by hydraulic drilling jar is directly applied to the drill string system. The axial direction is set as the origin of moment before the collision of hydraulic drilling jar, and the load acting on hydraulic drilling jar is 750kN. Remove nodes 50m and 100m from the drilling jar for single knock calculation respectively. The vibration displacement and velocity results of each node are shown in Figure 11.

By analyzing Fig. 11, with the increase of distance from the node to hydraulic drilling jar, the vibration displacement and velocity amplitude of drill string nodes gradually decreased, and the displacement and velocity amplitude at the installation of hydraulic drilling jar are the largest. Since the structure of drill string and the input conditions are unchanged, only the node positions are different, so the vibration frequency will not change. After 3s of the jarring force, the vibration displacement of three nodes is maintained at about 0.51m, and the vibration speed gradually stops. Therefore, in order to obtain a better effect of jar, it is necessary to install hydraulic drilling jar as close as possible to the stuck point.

The axial direction is set as origin of the moment before the collision of hydraulic drilling jar, and the down-jarring force acting on it is 400kN, 600kN and 800kN respectively, which is the lifting force calculated for single jarring calculation. The results of vibration displacement and vibration velocity at the node of hydraulic drilling jar are shown in Figure 12.

Analysis of Fig. 12 shows that with the increase of lifting force acting on hydraulic drilling jar, the vibration displacement of the node at hydraulic drilling jar increases significantly, and the displacement amplitude increases. The velocity amplitude will also increase with the increase of jarring force. After 3s of the jarring force, stop the vibration, and vibration displacement is 0.52m, 0.37m, 0.24m respectively. Therefore, in order to obtain a better effect of jar, it is possible to increase the force acting on hydraulic drilling jar. However, the bearing capacity of drill string system, downhole tools and location equipment is limited, so it is impossible to rely on unlimited increase of lifting force to enhance the effect of jar.

Keep the BHA (Bottom Hole Assembly) unchanged, the lifting force acting on hydraulic drilling jar is 750kN, and the moment before the collision of hydraulic drilling jar is set as the origin in the axial direction. The well depths of 3000m, 4000m and 5000m are taken as the single jarring calculation. The results of vibration displacement and velocity at

the node of hydraulic drilling jar are shown in Figure 13.

According to Fig. 13, with the increase of well depth, the vibration displacement and vibration velocity will increase, and the displacement and velocity amplitude will also increase. Due to the increase of well depth, which is equivalent to the increase of the length of upper drill string, under the same lifting force, the jarring load generated by hydraulic drilling jar will increase, and the effect of jar will be better. Therefore, the unlocking effect of deep wells is generally better than that of shallow wells. At the same time, with the change of drill string structure, the frequency of vibration displacement and velocity will also change.

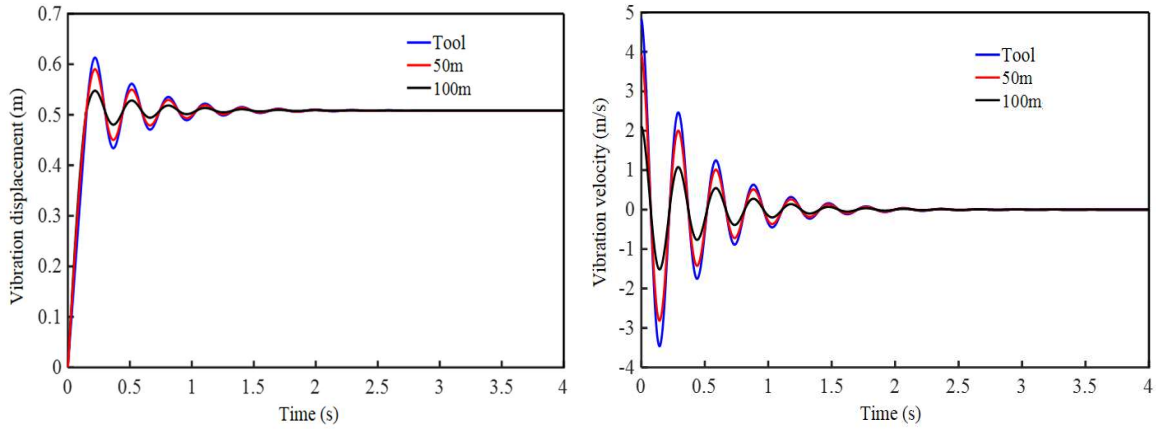

Fig. 11. Vibration displacement and velocity of different nodes

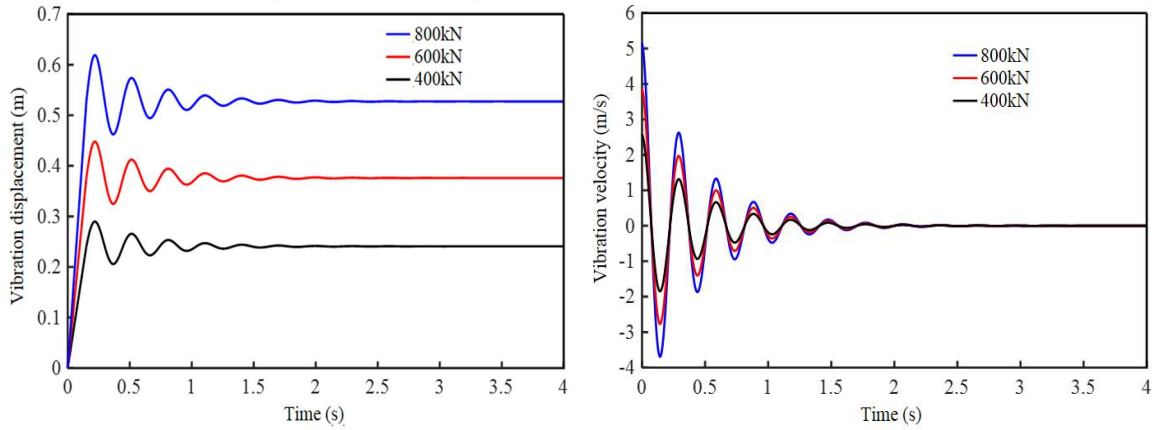

Fig. 12. Vibration displacement and velocity at hydraulic drilling jar under different lifting forces

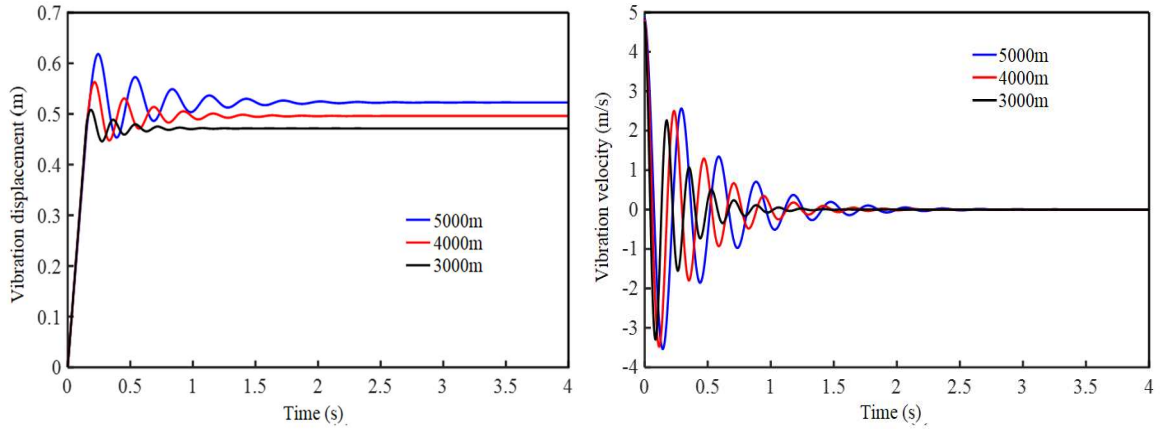

Fig. 13. Vibration displacement and velocity of hydraulic drilling jar at different well depths

Experimental test

In order to verify the feasibility of mechanical principle and whether the performance meets design requirements, the working performance of hydraulic drilling jar is further tested. The expansion and movement speed of hydraulic rod is set, and the tension or pressure of hydraulic rod of test system is

adjusted. The vibration data of hydraulic drilling jar is collected by the sensor, and the variation law of the upper and lower impact forces of hydraulic drilling jar is studied and analyzed to evaluate the working performance.

The tension and compression test bench of hydraulic drilling jar is shown in Figure 15, mainly includes a loading hydraulic cylinder console, a loading hydraulic cylinder and a clamping test bench. The combination of tension and compression test is hydraulic telescopic rod + upper connect + hydraulic drilling jar + lower connect. The experimental environment temperature is at room temperature indoors. The hydraulic oil used is the standard anti-wear hydraulic oil with ISO VG 46 viscosity, and the pressure adjustment range is 0-140Mpa. After the experimental combination is connected, the 30%-50% of maximum release force is designed to test stretching and compressing hydraulic drilling jar, and the expansion fluency of each connection and mandrel system is checked. Then install the test instrument and complete the installation and debugging of test instrument. The vibration test was conducted using an acceleration sensor in the experiment. The sensor was installed on a fixed platform and connected to the dynamic signal analysis system and the computer via data cables. Start the data acquisition system, transfer the acceleration signal collected by the acceleration sensor to the data acquisition card, and store it through the computer, as shown in Figure 14. The acceleration sensor used in the experimental test is the CA-YD-106 piezoelectric sensor, and its main technical indicators are shown in Table 3. During the experimental test, by loading the hydraulic cylinder console, the telescopic speed, tension and compression force of the telescopic rod of the loading hydraulic cylinder are controlled until the unlocking shock is completed.

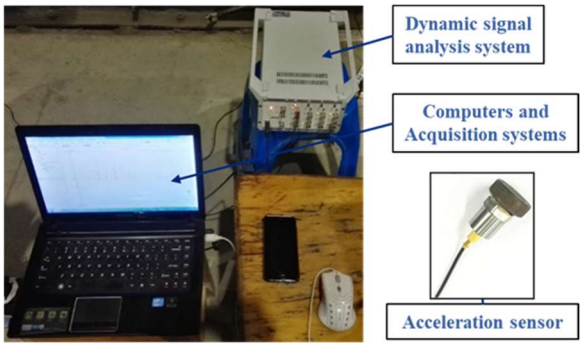

Fig. 14. Experimental testing equipment

By loading the hydraulic cylinder console, control the telescopic speed, tension and compression force until the jarring is completed.

After hydraulic drilling jar is assembled and inspected, it is shipped to the test site for experimental testing. Use the trolley to lift it horizontally into the tension and compression test bench. The drive mandrel of hydraulic drilling jar is connected to the telescopic rod of loading hydraulic cylinder through the upper connect, which can be moved in the direction of the drill follower axis on the tension and compression test bench, as shown in Figure 16.

Table 3. Main technical indicators of CA-YD-106 piezoelectric sensor

Project	Value
Axial sensitivity（20±5℃）	25pC/g
Peak value	2000g
Maximum lateral sensitivity	≤5%
Frequency response（±5%）	0.5~12000Hz
Working temperature range	-20~+120℃

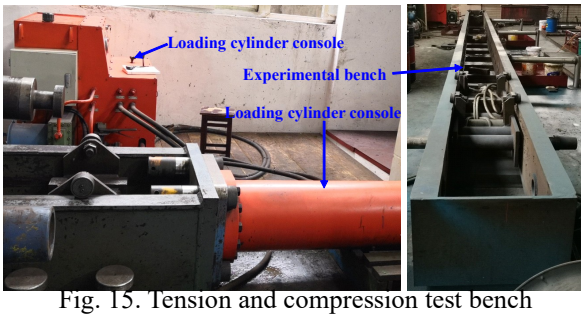

Fig. 15. Tension and compression test bench

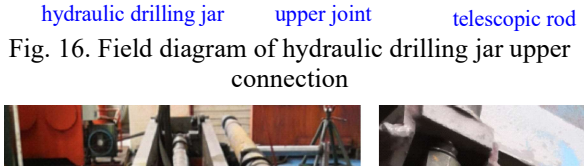

Fig. 16. Field diagram of hydraulic drilling jar upper connection

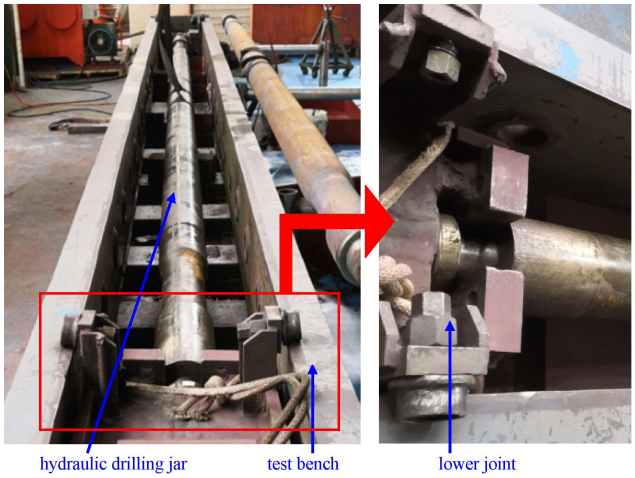

Fig. 17. Field diagram of hydraulic drilling jar lower connection

The lower joint of hydraulic drilling jar is

connected to the lower connect, and the lower connect is fixed to the tension and compression test bench. Therefore, during the experiment, the hydraulic cylinder system equivalent to hydraulic drilling jar is fixed with the tension and compression test bench, and cannot be moved to simulate the stuck drill situation, as shown in Figure 17.

According to the experimental equipment connection and layout diagram, the experimental combination is assembled, the connection of each part is checked, the preparation work is completed, and the experimental test of the drilling jar is carried out. The test steps and specific operations are as follows:

(1) By loading the hydraulic cylinder console, the moving speed of telescopic rod connecting the upper end of hydraulic drilling jar is set to 500mm/min~650mm/min. The tension of telescopic rod is adjusted to 30%~50% of the designed release force. Complete the operation of tensioning and compressing hydraulic drilling jar once, and check each connection part again.

(2) By loading the hydraulic cylinder console again, t the moving speed of telescopic rod connecting the upper end of hydraulic drilling jar is set to 500mm/min~650mm/min. The tension of telescopic rod is adjusted to 1.1 times of the designed release force. Complete three times of tensioning and compressing hydraulic drilling jar until unlocking the jar.

(3) According to the experimental equipment connection and layout diagram, the experimental data acquisition equipment is connected. The data connection line and test instrument are checked in the normal state, and the experimental test of hydraulic drilling jar is carried out.

(4) Set the moving speed of the telescopic rod is 500mm/min~650mm/min; set the tension of the telescopic rod to 400kN; start collecting data; and stop collecting after unlocking the shock.

(5) According to the above method, the tension of telescopic rod is set to 600kN and 800kN respectively, and the pressure of telescopic rod is set to 150kN, 250kN and 350kN respectively. The experiment is carried out and the data is collected. When testing the down-jar experiment, change the sensor direction.

(6) After the completion of experimental test, disassemble experimental equipment, and hydraulic drilling jar, and organize the experimental test equipment, clean up the experimental site, and complete the hydraulic drilling jar experiment.

The hydraulic drilling jar is placed on the tension and compression test bench for upward and downward impact experiments. At a speed of 500mm/min~650mm/min, 1.1×maximum allowable release force, the mandrel is pulled or pressed along the axis of hydraulic drilling jar. It can unlock the jar normally, and the delay time is greater than 30s. Conform to the design requirements. Due to the short length of mandrel, the elastic deformation is limited, but the tension or pressure acting on mandrel remains unchanged during the unlocking jarring process. Therefore, on the test bench, even if mandrel system produces a small elastic deformation, the jarring couple can still collide and produce a huge noise.

Through the analysis of collected experimental data, Figure 18 and Figure 19 are obtained. (a), (b), and (c) in Fig. 17 represent 400kN, 600kN, and 800kN tension of hydraulic telescopic rod acting on the mandrel system of hydraulic drilling jar, respectively. (a), (b), and (c) in Fig. 18 represent 150kN, 250kN, and 350kN pressure exerted by the hydraulic telescopic rod on the mandrel system of hydraulic drilling jar, respectively.

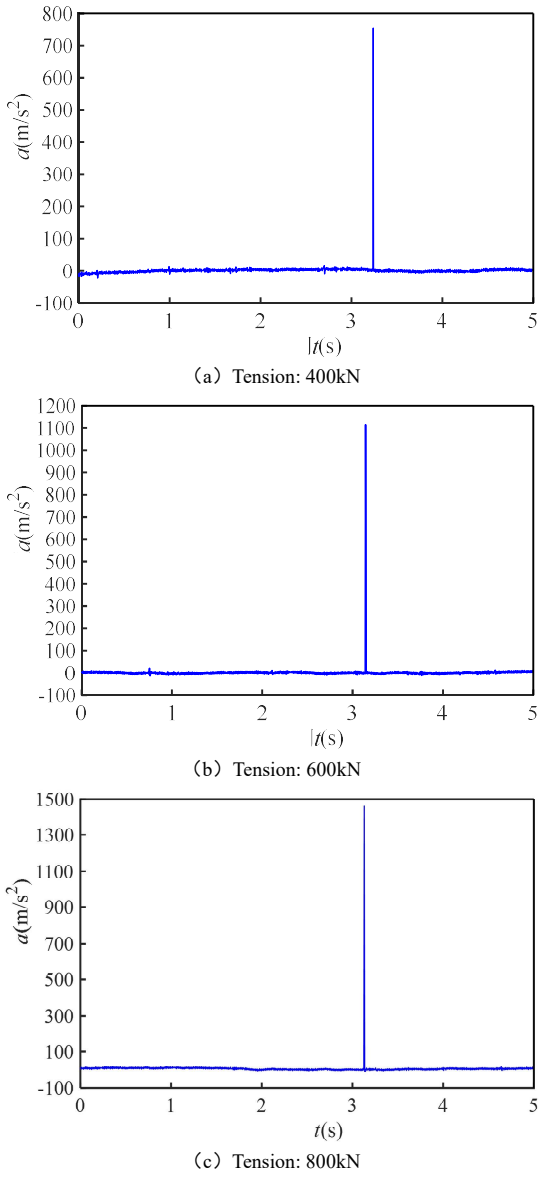

(a) Tension: 400kN

(b) Tension: 600kN

(c) Tension: 800kN

Fig. 18. Vibration acceleration of hydraulic cylinder system under different tension

In order to verify the accuracy, the theoretical calculation results are compared with experimental test results. Through the relative error calculation formula,

the relative error between the experimental value and the theoretical calculation value of each experimental test point is calculated respectively.

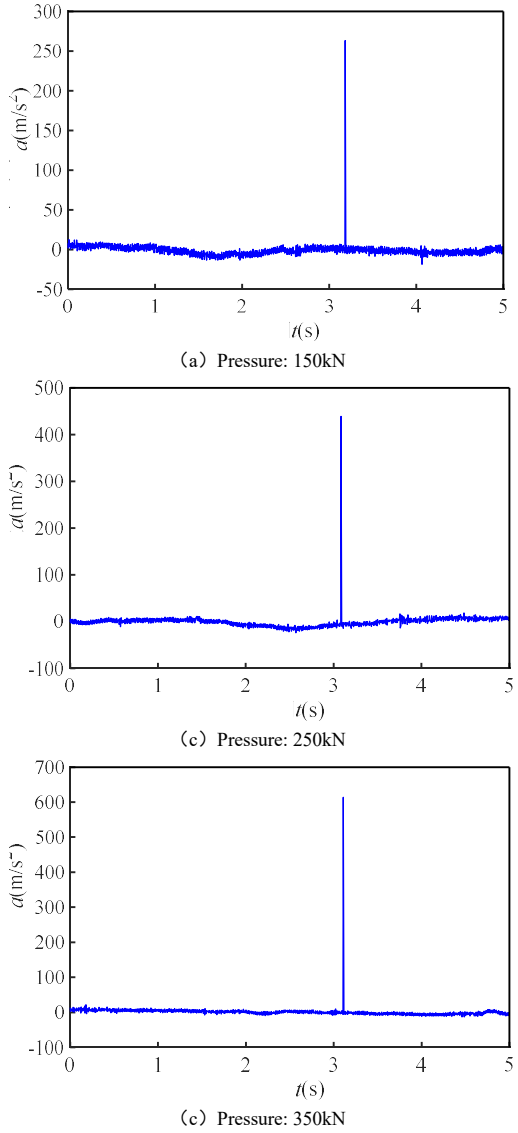

Fig. 19. Vibration acceleration of hydraulic cylinder system under different pressure

By observing and analyzing Figure 20 and Figure 21 respectively, it can be seen that the maximum relative error between theoretical calculation results and experimental values of upper impact collision force is 6.9616%, and the average relative error is 5.6185%. When only the tensile force acting on the mandrel system of hydraulic drilling jar is changed. Change the pressure acting on the mandrel system of hydraulic drilling jar, the maximum relative error between the theoretical calculation result and experimental value of lower impact collision force is 6.7199%, and the average relative error is 6.85%. From the comparison between theoretical calculation results and experimental values of impact force, it can be seen that when the parameters changed are the same, the trajectory trends changed are the same. The release force increases linearly with the increase of the tension or pressure, and the error is less than 10%. Therefore, the reliability of theoretical calculation results is explained, and the relative error mainly comes from the simplification of theoretical calculation model. In the theoretical calculation, there is only the conversion of kinetic energy and elastic potential energy during the process. The theoretical calculation value ignores the deformation caused by the collision, and the conversion loss of damping and internal energy is ignored.

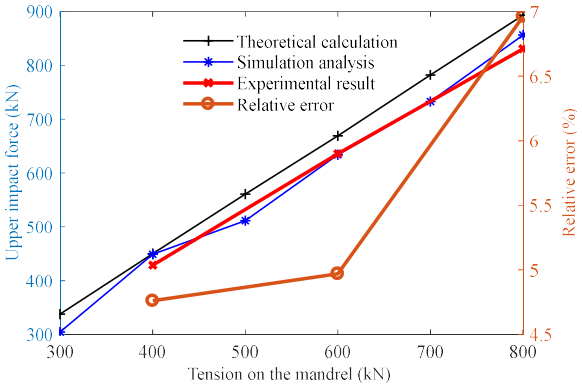

Fig. 20. Comparison of theoretical calculation results and experimental values of upper impact force

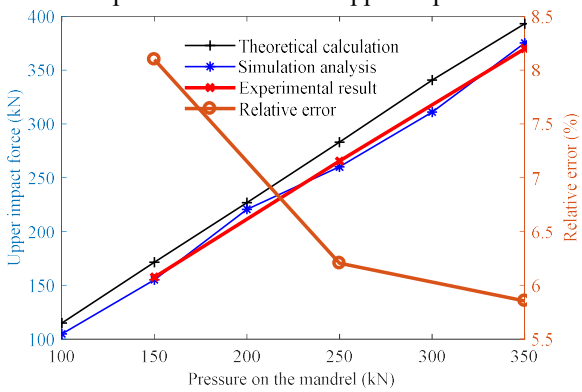

Fig. 21. Comparison of theoretical calculation results and experimental values of lower impact force

Conclusion

In this paper, design a kind of hydraulic drilling jar, introduce its working mechanism and performance characteristics in detail, and carry out working characteristics and dynamic analysis. Finally, experimental tests are carried out.

By establishing a theoretical model for the mandrel system's force and jarring impact force, we conducted simulations of the jarring force using ADAMS software. Subsequently, a comparative analysis was performed between the theoretical calculation value and simulation results. The maximum relative error between theoretical calculation and simulated value of the upper impact collision force is 9.8621%, and the average relative error is 5.7665%; the maximum relative error between theoretical calculation and experimental value of lower impact collision force is 9.6123%, and the average

relative error is 7.1042%. All are within reasonable range of relative error.

The dynamics model is carried out for the combination of drilling tools equipped with hydraulic drilling jar, and the analysis is combined with the jarring load results of drilling string and relevant parameter calculations. The results of axial vibration displacement and velocity are obtained with different node positions, lifting forces and well depths. In order to obtain better vibration unlocking effect, hydraulic drilling jar can be installed as close to the stuck point as possible, and increasing the vibration force acting on hydraulic drilling jar. At the same time, the unlocking effect of deep wells will be better than that of shallow wells.

Finally, the experimental verification is conducted to complete the tensile and compression experiments of both upstroke and downstroke generated by the drilling jar. The maximum relative error between theoretical calculation results and experimental values of upper impact collision force is 6.9616%, and the average relative error is 5.6185%. Change the pressure acting on the mandrel system of hydraulic drilling jar, the maximum relative error between the theoretical calculation result and experimental value of lower impact collision force is 6.7199%, and the average relative error is 6.85%.

After the comparative analysis, the theoretical calculation of upward and downward impact force is within the tolerance range of error, which is consistent with simulated value and experimental results. The test results verify the correctness of theoretical calculation to a certain extent, which is a further test of the working performance of hydraulic drilling jar and can provide some guidance for the subsequent structural optimization.

Declaration of conflicting interests

The author(s) declared no potential conflicts of interest with respect to the research, authorship, and/or publication of this article.

Funding

The author(s) disclosed receipt of the following financial support for the research, authorship, and/or publication of this article: This work was funded by Science and Technology Innovation Fund, Chengdu, China (2022-RC03-00005-CG), State Key Laboratory of Gas Disaster Monitoring and Emergency Technology, China (2021SKLKF07).

Reference

Aarrestad, T.V., Kyllingstad, A., "Loads on Drillpipe During Jarring Operations," SPE Drilling & Completion, Vol. 9, pp. 271-275 (1994). DOI: 10.2118/24970-PA.

Askew, W.E., "Computerized Drilling Jar Placement," Proc. of IADC/SPE Drilling Conference, Dallas, Texas (1986). DOI: 10.2118/14746-MS.

Deng, R., Xi, H., Huang, C., "Jar by Finite Element Analysis of Dynamic Load," Oil Field Machinery, Vol. 38, No. 9, pp. 1-3 (2009). DOI: 10.3969/j.issn.1001-3482.2009.09.014.

Fan, C., Li, X., Zhou, J., "Optimization Design of Damping Mechanism for Hydraulic Impact Device," Mechanical Manufacturing, Vol. 51, No. 6, pp. 76-78 (2013).

Feng, W., Li, Q., Ji, G., Fu, Y., Liu, Y., "The Application of Bidirectional Hydraulic Vibrator in Tarim Oilfield," Petrochemical Technology, Vol. 31, No. 4, pp. 66-68 (2024).

Guo, J., Liu, G., Zhang, G., Li, D., "While Drilling Jar and Shock Absorber Failure Analysis and Solution," Journal of Petroleum Machinery, Vol. 37, No. 12, pp. 1-4 (2009). DOI: CNKI:SUN:SYJI.0.2009-12-025.

Han, J., Sun, H., "Double-Acting Mechanical Hydraulic Jar with Drilling," Journal of Development and Application of Petrochemical Technology, Vol. 22, No. 8, pp. 147-163 (2015). DOI: 10.3969/j.issn.1006-0235.2015.08.109.

Hu, H., "Development and Application of Hydraulic Continuous Jarring Absorber," Journal of Jianghan Petroleum Workers' University, Vol. 29, No. 2, pp. 70-72 (2016).

Jin, Z., Liang, X., "Exploration and Development of Shale Oil in China: State, Challenges, and Prospects," Russian Geology and Geophysics, Vol. 65, No. 1, pp. 20-34 (2024). DOI: 10.2113/RGG20234647.

Kalsi, M.S., Wang, J., Chandra, U., "Transient Dynamic Analysis of the Drillstring Under Jarring Operations by the FEM," SPE Drilling Engineering, Vol. 2, pp. 47-55 (1987). DOI: 10.2118/13446-PA.

Kelly, L.W., "Technical Problems and Measures of Wellbore Stability of Broken Formation in Shunbei Oil and Gas Field," Science Technology & Engineering, Vol. 22, No. 13, pp. 5205-5212 (2022). DOI: 10.1080/10286632.2015.1015532.

Li, P., "Simulation of Longitudinal Vibration Characteristics of Drill String and Unstuck Effect of Jar in Vertical Well," Ph. D. Thesis, Yanshan University, Qinhuangdao, China (2019).

Li, X., "Application of Jar While Drilling in Drilling," Western Exploration Engineering, Vol. 31, No. 6, pp. 65-68 (2019).

Li, Z., Zhang, Y., Hou, X., Liu, W., Xu, G., "Analysis of Longitudinal and Torsional Vibration of Drill String," Engineering Mechanics, Vol. 21, No. 6, pp. 203-208 (2004).

Li, J., "Mechanical Locking Hydraulic Drilling Jar Application Analysis," Oil Field Machinery, Vol. 35, No. 7, pp. 1-4 (2014). DOI: 10.3969/j.issn.1001-3842.2014.07.017.

Liu, C., Lv, R., Li, H., He, J., "Hydraulic Jar on Bench Test Dynamics Study," Oil Field Machinery, Vol.

37, No. 7, pp. 1-4 (2008). DOI: 10.3969/j.issn.1004-4388.2008.04.004.

Liu, C., Luo, J., Zhang, J., "Rayleigh Calculation Method of Hydraulic Jar Load," Inner Mongolia Petrochemical Industry, Vol. 29, No. 11, pp. 108-110 (2008). DOI: 10.3969/j.issn.1006-7981.2008.11.049.

Mao, L., Zou, D., Chen, G., "Drilling Fluid Technology for Puqian 12-Ping 1 Ultra-Shallow Viscous-Oil Horizontal Well," Oil Drilling & Production Technology, pp. 1-10 (2015). DOI: 10.13639/j.odpt.2015.04.014.

Mcgill, H., Dalton, C., "Analytical and Experimental Investigation of Flow in a Hydraulic Jar," Society of Petroleum Engineers Journal, Vol. 8, No. 4, pp. 351-358 (1968). DOI: 10.2118/2118-PA.

Newman, K.R., Procter, R., "Analysis of Hook Load Forces During Jarring," Proc. of SPE Annual Technical Conference and Exhibition, pp. 1-10 (2009). DOI: 10.2118/118435-MS.

Pan, Z., Song, S., Wang, X., Huang, Y., Zhu, L., Li, N., "While Drilling Jar Joint Fracture Analysis and Improvement Measures," Oil Drilling Technology, Vol. 32, No. 6, pp. 1-4 (2010). DOI: 10.3969/j.issn.1000-7393.2010.06.031.

Skeem, M.R., Friedman, M.B., and Walker, B.H., "Drillstring Dynamics During Jar Operation," Journal of Petroleum Technology, Vol. 31, pp. 1381-1386 (1979). DOI: 10.2118/7521-PA.

Sun, R., Huang, B., "Calculation of Upward Jarring Load of Oil Drilling Tool," China Petroleum Machinery, Vol. 25, No. 5, pp. 4-8 (1997).

Tian, J., Song, J., Zhong, L., Liu, Y., He, Y., "Research on Dynamics and Performance of Composite Impact Acceleration Tool," Journal of Vibration Engineering & Technologies, pp. 1-13 (2023). DOI: 10.1007/s42417-023-00943-3.

Tian, J., Yang, Y., Dai, L., Song, H., Gong, X., Li, J., " Dynamic mechanism of fluidic oscillation of a new friction reducing tool," Natural Gas Industry, Vol. 39, No. 5, pp. 99-106 (2019). DOI: 10.3787/j.issn.1000-0976.2019.05.012

Yin, H., Luo, N., Li, Q., "Analysis of Hydraulic Jarring Dynamics and Calculation of Impact Force," Applied Mechanics and Materials, pp. 129-134 (2014). DOI: 10.4028/www.scientific.net/amm.577.129.

Zhang, Y., Chen, P., "Study of Drilling Jar," Oil Field Machinery, Vol. 27, No. 4, pp. 1-3 (1998). DOI: CNKI:SUN:SKJX.0.1998-04-002.

Zhao, Y., "Research on Longitudinal Vibration of Drilling String in Horizontal Wells," Master's Thesis, Daqing Petroleum Institute, Daqing, China (2007).